Pergamon

Bioorganic & Medicinal Chemistry, Vol. 4, No. 1, pp. 121–129, 1996

0968-0896/96 $15.00+0.00

0968-0896(95)00176-X

MS-271, A Novel Inhibitor of Calmodulin-Activated Myosin Light Chain Kinase from *Streptomyces* sp.—II. Solution Structure of MS-271: Characteristic Features of the 'Lasso' Structure

Ritsuko Katahira, Motoo Yamasaki, Yuzuru Matsuda and Mayumi Yoshida*

Tokyo Research Laboratories, Kyowa Hakko Kogyo Co. Ltd, 3-6-6 Asahimachi, Machida-shi, Tokyo 194, Japan

Abstract—MS-271 is a potent inhibitor of smooth muscle myosin light chain kinase (MLCK), obtained from *Streptomyces* sp. In the previous paper, we reported on the isolation, structural determination and biological properties of MS-271.[1] In this paper, we report on the three-dimensional structure of MS-271 determined by ^{1}H NMR in deuterated dimethyl sulphoxide. MS-271 consists of 21 amino acid residues with a novel internal linkage between the β-carboxyl group of Asp9 and the α-amino group of Cys1, and two disulfide bonds, Cys1–Cys13 and Cys7–Cys19. The internal linkage between the side chain of Asp9 and the α-amino group of the N-terminal residue is the same as that of the endothelin B receptor selective antagonist, RES-701-1, that we previously reported. The structural calculations involved the combined use of distance geometry and simulated annealing calculations. The results indicated that MS-271 undergoes extraordinary folding, i.e. the 'tail' (Phe10–dTrp21) passes through the 'ring' region (Cys1–Asp9) ('lasso' structure). This folding of MS-271 turned out to be the same as the 'lasso' structure of RES-701-1. The features of this 'lasso' structure are discussed on the basis of comparison between the structures of MS-271 and RES-701-1.

Introduction

Myosin light chain kinase (MLCK) is one of the key regulatory enzymes in Ca^{2+} dependent responses.[2,3] The kinase catalyzes the transfer of the γ-phosphate of ATP to the 20-kDa myosin light chain (MLC).[3] Specific inhibitors of MLCK are expected to be not only good tools for investigating the actual function of the enzyme but also to be potential pharmacological agents, such as vasodilators and anti-inflammatory agents. Recently, we isolated a novel MLCK inhibitor, MS-271 (IC_{50}=8 μg/ml),[1] from *Streptomyces* sp. Its amino acid sequence is shown in Figure 1. The primary structure of MS-271 was determined by the sequencing of peptide fragments obtained by limited chemical hydrolysis, FABMS and NMR spectroscopy.[1] This inhibitor is composed of 21 amino acid residues and possesses a novel primary structure, i.e. an internal linkage between the β-carboxyl group of Asp9 and the α-amino group of Cys1, and two disulfide bridges, between Cys1 and Cys13, and Cys7 and Cys19. Recently, anti-HIV protein RP 71955 was obtained from *Streptomyces*.[4,5] The amino acid sequence of MS-271 is similar to those of RP 71955 (Fig. 1) and siamycin II and the same as that of siamycin I, as recently published.[6] To aid understanding, we have named the Cys1–Asp9 region the 'ring' and the Phe10–Trp21 region the 'tail'. We previously determined the solution structure of the endothelin B receptor (ET_B) selective antagonist, RES-701-1, which possesses the same internal linkage as MS-271 (siamycin I), RP 71955 and siamycin II (Fig. 1).[7,8] We revealed that RES-701-1 undergoes extraordinary folding, i.e. the 'tail' passes through the 'ring' ('lasso' structure). Until now, two other peptides which possess the same internal linkage as MS-271 (siamycin I), siamycin II, RP 71955 and RES-701-1, were known. One is the atrial natriuretic peptide, anantin[9] (Fig. 1) and the other is the inhibitor of prolyl endopeptidase, peptide propeptin[10] (Fig. 1), although the 3-D structures of these peptides have not yet been reported. In this study, we elucidated the 3-D structure of the MLCK inhibitor, MS-271, based on ^{1}H NMR and combined distance geometry (DG) and simulated annealing (SA) calculations. The resulting structure was compared with the solution structure of the ET_B selective antagonist, RES-701-1, in detail, which possesses the same internal linkage as MS-271. In addition, we discussed the characteristic features of the 'lasso' structure. The solution structure of MS-271 was also compared with those of the anti-HIV peptide, RP 71955, determined by Frèchet et al.[5] and siamycin II, determined by Constantine et al.[11]

Key words: MLCK, inhibitor, ^{1}H NMR, distance geometry, simulated annealing, lasso structure.

Results

Sequential assignments and secondary structure elements

All the experiments were carried out in a DMSO solution. Assignments of the proton resonances were

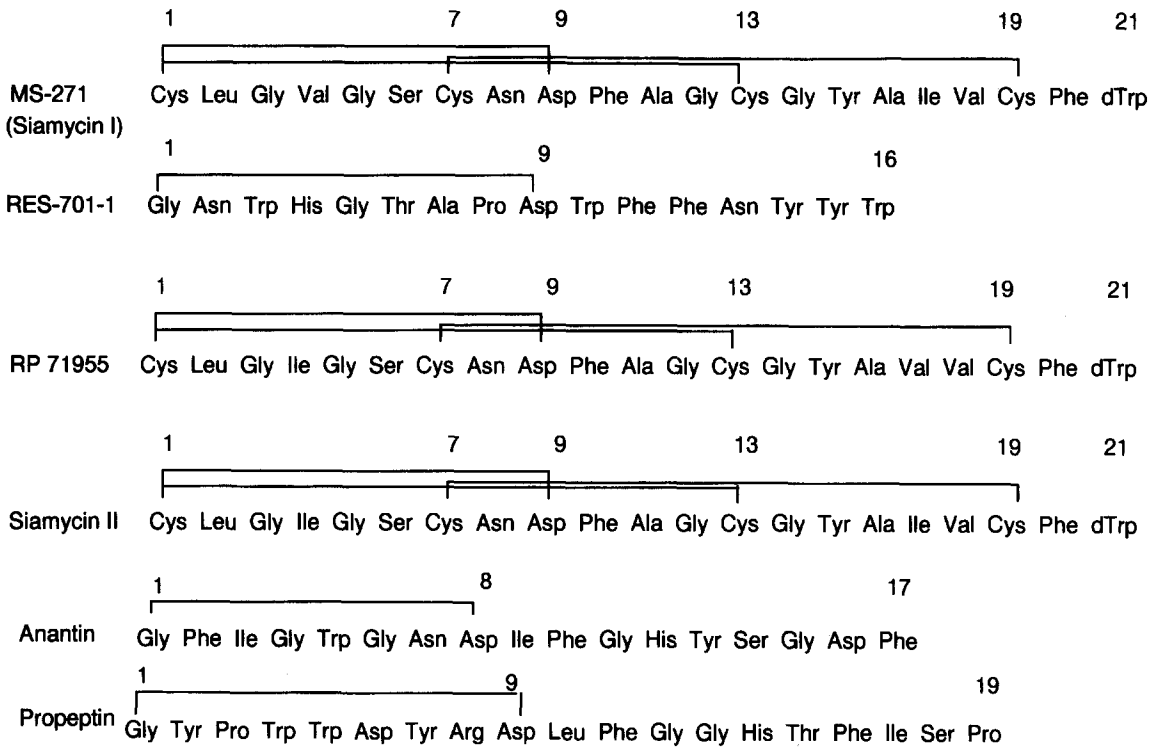

Figure 1. Amino acid sequences of MS-271 (siamycin I), RES-701-1, RP 71955, siamycin II, anantin and propeptin.

performed by means of the sequence specific assignment strategy of Wüthrich.[12] The proton chemical shifts of MS-271 are listed in Table 1. The sequential and longer range NOEs are summarized in Figure 2. Strong sequential $d_{\alpha N}$ NOEs were observed for the Cys7–Asp9 and Gly14–Ala16 segments. A strong $d_{\alpha\alpha(i,j)}$ NOE between the CαHs of Asn8 and Tyr15 and strong $d_{\alpha N(i,j)}$ NOEs between the CαH of Tyr15 and the NH of Asp9, and the CαH of Asn8 and the NH of Ala16 were observed (Fig. 2). These NOEs reveal the presence of an antiparallel β-sheet structure between the Cys7–Asp9 and Gly14–Ala16 segments. The $d_{\alpha\beta(i,j)}$ NOE between the CαH of Ala16 and the CβH of Leu2, and the $d_{\beta N(i,i+2)}$ NOE between the CβH of Leu2 and the NH of Val4 suggest the interaction between the side chain atoms of Leu2 and the backbone atoms of Val4 and Ala16. In addition, several NOEs were observed between the side chain of

Table 1. ^{1}H chemical shifts of MS-271 in DMSO at 303 K

Number	NH	CαH	CβH	Others
C1	8.5	4.58	2.58, 3.50	
L2	9.29	4.50	1.58, 2.14	γH 2.03 δMe 1.03, 0.93
G3	9.12	4.14, 3.58		
V4	6.67	4.47	1.78	γMe 0.7, 0.77
G5	7.88	4.43, 3.35		
S6	7.62	4.38	3.58, 3.73	γ4.95
C7	7.83	4.65	3.18, 3.32	
N8	8.83	5.16	2.23, 2.28	
D9	7.92	4.38	3.58, 3.73	
F10	8.01	4.26	2.72	H2,5 7.25, H3,5 7.25, H4 7.21
A11	8.70	3.89	1.14	
G12	8.75	3.89, 3.39		
C13	8.10	4.30	2.83, 3.42	
G14	7.26	2.98, 3.52		
Y15	9.06	5.37	2.80, 1.93	H2,6 6.77, H3,5 6.47
A16	8.21	4.60	1.17	
I17	8.06	4.41	1.93	ϕH 1.39, 1.06, ϕMe 0.83, δMe 0.79
V18	6.92	4.14	1.84	γMe 0.83, 0.79
C19	8.20	4.47	2.57, 280	
F20	7.61	4.59	2.60, 2.78	H2,6 6.91, H3,5 6.91, H4 7.03
W21	8.42	4.46	2.98, 3.20	H2 7.16, H4 7.57, H5 7.00, H6 7.08, H7 7.34, NH 10.84

Tyr15 and the backbone of the Gly3–Gly5 segment. The $d_{\beta N(i,j)}$ NOE between the CβH of Tyr15 and the NH of Gly5, the $d_{\beta N(i,j)}$ NOE between the CβH of Tyr15 and the NH of Val4, the $d_{\alpha\beta(i,j)}$ NOE between the CαH of Gly5 and the CβH of Tyr15 and the $d_{\alpha\varepsilon(i,j)}$ NOE between the CαH of Gly3 and the CεH of Tyr15 suggest that the side chain of Tyr15 is close to the backbone atoms of the Gly3–Gly5 segment of the 'ring'.

Determination of the three-dimensional structure

After the DADAS calculations, 40 of the 100 structures with best-satisfied NMR restraints were used for further SA refinement. Figure 3 shows the backbone atoms of 35 refined structures of MS-271. This figure shows that MS-271 undergoes extraordinary folding, i.e. the 'tail' region passes through the 'ring' region. Table 2 shows the energy statistics and rms values for MS-271. For the 35 accepted structures among the 40 calculated ones, the distance constraint violations were less than 0.1 Å and the angle constraint violations were less than 5 degrees. Figure 4 shows the average rms per residue for the 35 accepted structures. The backbone atoms for residues 1–20 are well defined. Systematic analysis of the obtained structures was undertaken using the φ and ψ dihedral angles determined with the program X-PLOR. Figure 5 shows the Ramachandran plot of the 35 SA structures. The φ and ψ angles of the residue which exhibit high rms values in Figure 4 are also diverse dihedral ones. In Figure 5, the ψ and φ angles of Cys7, Asn8, Asp9, Gly14, Tyr15, and Ala16 can be seen to reside in the range of the β-sheet region shown in Figure 4.

Discussion

The 'lasso' structure of MS-271 and the key NOE patterns which reflect the 'lasso' structure in general

We have determined the three-dimensional structure of the MLCK inhibitor, MS-271. The results indicated above show that MS-271 adopts an extraordinary structure, i.e. the 'tail' passes through the 'ring' region. Figure 6 shows a ribbon representation of the average structure of the accepted 35 SA structures of MS-271. It shows that the Gly14–Tyr15 segment of the 'tail' lies above Cys1–Leu2 of the 'ring' and the Ala16–Tyr15 segment of the 'tail' lies below Gly5–Cys7 of the 'ring'. The relative position of the Gly14–Tyr15 segment as to the Cys1–Leu2 segment, and that of the Tyr15–Ala16 segment as to the Gly5–Ala7 segment could be defined directly on the basis of the critical NOEs observed, as demonstrated below. The Cys7–Asp9 and Gly14–Ala16 segments form a β-sheet structure, as discussed under Results. In the β-sheet structure, the side chains of two consecutive residues stick out in opposite directions with respect to the backbone ribbon in the β-sheet

Figure 2. NOE connectivities and coupling constants of MS-271. The thickness of bars indicates the intensity of NOE cross peaks. For temperature coefficients, open circles indicate that $5 \leq \Delta\delta/\Delta T$, filled circles, that $3 \leq \Delta\delta/\Delta T < 5$, filled squares, $V < 3$ ppb/K. For coupling constants, filled squares indicate that $J \geq 9$ Hz, and open circles, that $J < 5$ Hz. $d_{\alpha N(i,j)}$, $d_{\alpha\alpha(i,j)}$, and $d_{NN(i,j)}$ denote the NOEs between the i and j residues.

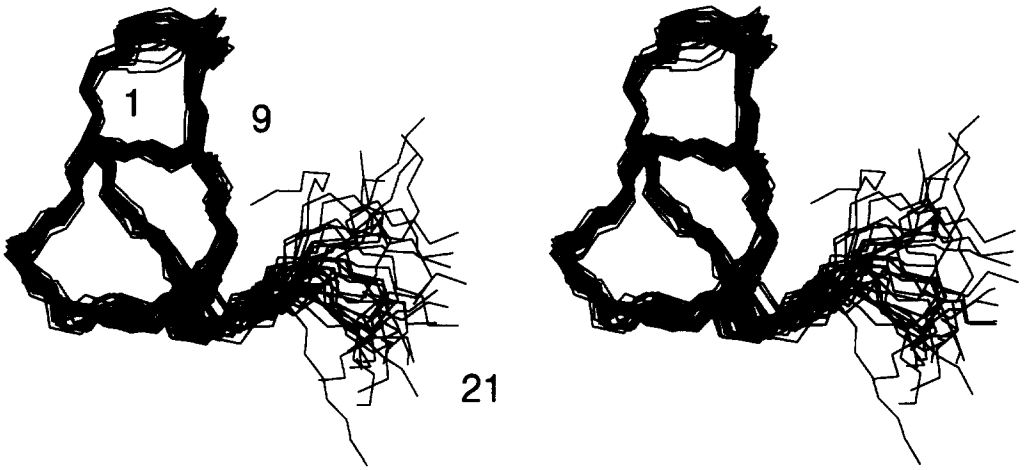

Figure 3. Stereoview of backbone atoms (N, Cα, C) and the linkage carbons (Cβ and Cγ of Asp9) of a family of 35 structures for MS-271. The structures were each superimposed for minimum pairwise rms values of the backbone atoms.

Table 2. Energy statistics of 35 SA structures for MS-271

X-PLOR potential energy	
Etotal (kcal mol^{-1})	2.17±0.35
Ebond	0.27±0.03
Eangle	0.84±0.16
Eimproper	0.42±0.02
Evdw	0.18±0.15
ENOE	0.43±0.11
Ecdih	0.02±0.01
Rms from the idealized geometry within X-PLOR	
bonds (Å)	0.00±0.00
angles (degree)	0.12±0.05
impr (degree)	0.13±0.02
Rms from experimental restraints	
NOE (Å)	0.00±0.00
cdih (degree)	0.18±0.14
Rms	
backbone (1–19)	0.71±0.11
heavy atoms (1–19)	1.12±0.35

structure. Thus, the side chain of Asp9, which is the next residue to Asn8, is below the backbone ribbon of the Cys7–Asp9 segment. Since the side chain of Asp9 is linked with Cys1, the Cys1–Leu2 segment could not be above the backbone ribbon of the antiparallel β-sheet segment shown in Figure 6. Therefore, the Gly14–Tyr15 segment must be above Cys1–Leu2. Several NOEs were observed between the side chain of Tyr15 and the backbone atoms of the Gly3–Gly5 segment of the 'ring' (Figure 6, dotted lines), as indicated under Results. These NOEs suggested that the side chain of Tyr15 is close to the backbone of the Gly3–Gly5 segment of the 'ring'. As discussed above, the Gly14–Tyr15 segment lies above the Cys1–Leu2 segment. If one tries to put the side chain of Tyr15 close to the backbone protons of the Gly3–Gly5 segment under these circumstances, the Tyr15–Ala16 segment must be located below the Gly5–Cys7 segment to avoid steric hindrance from the extending backbone of the Tyr15–Ala16 segment. Thus, the relative position of the Ala16–Tyr15 segment as to the Gly5–Cys7 segment can be defined in this way. In

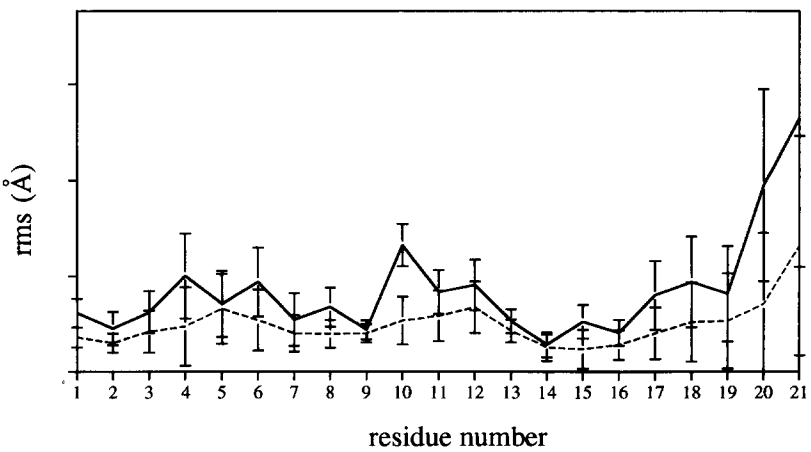

Figure 4. Average rms of the structures refined with the program X-PLOR. The dashed line indicates backbone atoms and the solid line, heavy atoms.

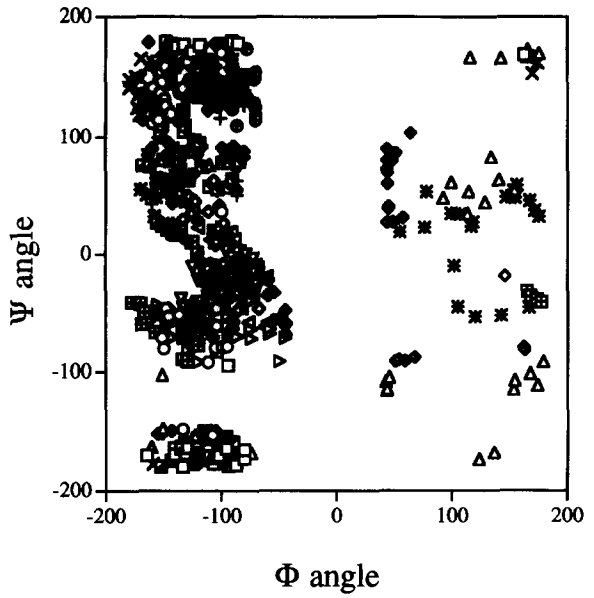

Figure 5. Ranachandran plot of the 35 SA family of MS-271. The legend is (□) L2, (◇) G3, (○) V4, (△) G5, (⊞) S6, (⊕) C7, (⊕) N8, (▽) D9, (◪) F10, (►) A11, (*) G12, (▷) C13, (◩) G14, (◈) Y15, (×) A16, (◁) I17, (⧅) V18, (⊖) C19, (+) F20.

summary, the Gly14–Tyr15 segment of the 'tail' lies above the Cys1–Leu2 segment of the 'ring', and after passing through the 'ring', the Ala16–Tyr15 segment of the 'tail' lies below the Gly5–Cys7 segment of the 'ring'. Again the 'lasso' structure was deduced directly on the basis of the critical NOEs, as indicated in the previous report on the structure of RES-701-1.

We previously reported on the solution structure of the ET_B selective antagonist, RES-701-1, which possesses the same internal linkage as MS-271, between the β-carbonyl carbon of Asp9 and the α-amino group of the N-terminal residue. The folding of RES-701-1 involving passing of the 'tail' through the 'ring' region ('lasso' structure). In addition, RP 71955 and siamycin II, of which the amino acid sequences are similar to that of MS-271, were reported to adopt a 'lasso' structure similar to that of RES-701-1.[7] Then we discussed the key NOE patterns which reflect the 'lasso' structure on the basis of the results of NMR studies on RES-701-1 and MS-271. The NOEs which indicate a β-sheet structure were commonly observed for MS-271 and RES-701-1 for two segments (Cys7–Asp9 and Gly14–Ala16 in MS-271 and Ala7–Asp9 and Phe12–Tyr14 in RES-701-1). In addition to this, as indicated above, several critical NOEs were observed between the backbone protons of the 4–5 segment and the side chain of the middle residue of the β-sheet in the 'tail' region (Tyr15 in MS-271, and Asn13 in RES-701-1). In conclusion, a peptide consisting of the RES-701-1-type 'ring' and the 'tail' will adopt the 'lasso' structure, i.e. the 'tail' passes through the 'ring', if the following two NOE patterns are observed: 1. NOEs which reflect the antiparallel β-sheet between the 7–9 segment of the 'ring' and the 'tail'; 2. NOEs between the backbone protons of the 4–5 segment of the 'ring' and the side chain of the middle residue of the β-sheet segment in the 'tail'.

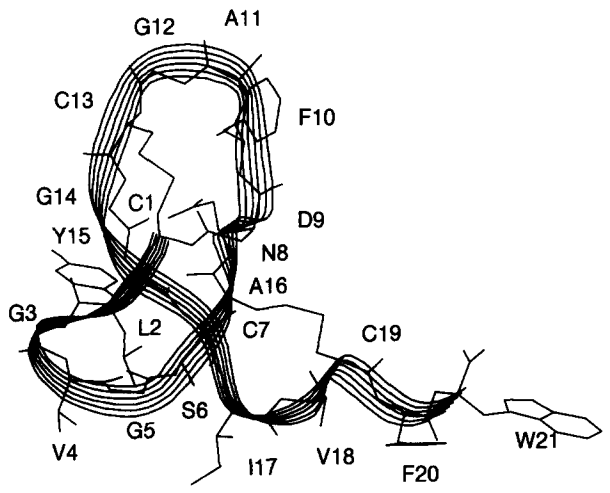

Figure 6. Ribbon representation of MS-271. For the dotted lines, see the text.

The characteristic features of the 'lasso' structure

In the previous report, we suggested that the 'lasso' structure of RES-701-1 determined by us is the first example of a knot structure in which metal atoms are not included in the formation of the knot structure.[7] Here we suggest the features of this 'lasso' structure, in detail, on the basis of comparison of the structures of MS-271 and RES-701-1.

One segment of the β-sheet structure consists of the 7–9 segment of the 'ring' region in both peptides. Therefore it is suggested that the linkage from the β-carboxyl carbon of Asp9 to the α-amino group of the N-terminal residue defines the structure of that segment, as also indicated in the previous report.

In RES-701-1, it was found that a hydrogen bond was formed between the NH of Asn13 in the 'tail' and the CO of Asn2 in the 'ring'. In RES-701-1, a β-sheet structure is formed between the segments of Ala7–Asp9 and Phe12–Tyr14. The amide proton of Asn13, which is the middle residue of the β-sheet region in the 'tail', is flipped out in the opposite direction with respect to that of the amide protons involved in the hydrogen-bonding in the β-sheet structure. However, since the 'tail' passes through the 'ring', the NH of Asn13 is hydrogen bonded to the CO of Asn2. This fact was also supported by the low temperature coefficient value of Asn13. Therefore the hydrogen bond between the NH of Asn13 and the CO of Asn2 was found to be a characteristic feature of the 'lasso' structure.[7] For MS-271, it was also found that a hydrogen bond is formed between the amide proton of Tyr15 and the carbonyl oxygen of Leu2, since the distance between these atoms is only 2.5 Å. Under the circumstances of the presence of a β-sheet structure between segments 7–9 and 14–16, this hydrogen bond will never be formed unless the 'tail' passes through the 'ring'. The susceptibility to temperature of the

amide proton chemical shifts of MS-271 is shown in Figure 2. The susceptibility to temperature of the amide proton chemical shifts of Cys7, Asp9, Gly14 and Ala16 are low since these atoms are involved in the hydrogen bonds in the β-sheet structure. In addition, that of Tyr15 is also low. Thus, the presence of the hydrogen bond between the NH of Tyr15 and the CO of Leu2 was supported by the low amide proton temperature coefficient value of Tyr15. In conclusion, a hydrogen bond between the carbonyl oxygen of residue 2 and the amide proton of the middle residue of the β-sheet region in the 'tail' was commonly observed for MS-271 and RES-701-1. It is suggested that the backbone folding of the 'lasso' structure would be stabilized by this hydrogen bond.

In order to examine the structure which is commonly observed for RES-701-1 and MS-271, the 'core' structure, fitting of the two structures was performed. Figure 7 shows the superimposed structures of RES-701-1 and MS-271. Fitting was accomplished with respect to the Cα carbons of the 'ring' (1–9) and the β-sheet segment of the 'tail' (14–16 of MS-271 and 12–14 of RES-701-1). The rms between RES-701-1 and MS-271 was 0.4 Å, indicating that the backbone structures of the fitted region are highly conserved. In addition, the orientation of the side chain of Tyr15 in MS-271 is similar to that of Asn13 in RES-701-1 (both residues are the central residue of the β-sheet in the 'tail') and the orientation of the side chain of Leu2 in MS-271 is similar to that of Asn2 in RES-701-1, although the fitting was only performed for the backbone Cα atoms. The orientation of the side chains of these residues is well defined (Fig. 5). The orientation of the side chain of Tyr15 is defined by the NOEs between the side chain of Tyr15 and the backbone protons of the 3–5 segment and that of Asn13 by the NOEs between the side chain of Asn13 and the backbone protons of the 4–5 segment, as indicated above. In addition, the orientation of Leu2 in MS-271 is defined by the NOEs between the CβH of Leu2 and the backbone protons of His4 and Ala16 and that of Asn2 in RES-701-1 is defined by the NOEs between the side chain of Asn2, and the backbone protons of His4 and Tyr14. Residue Ala16, which is the next residue to Tyr15 in the β-sheet of MS-271,

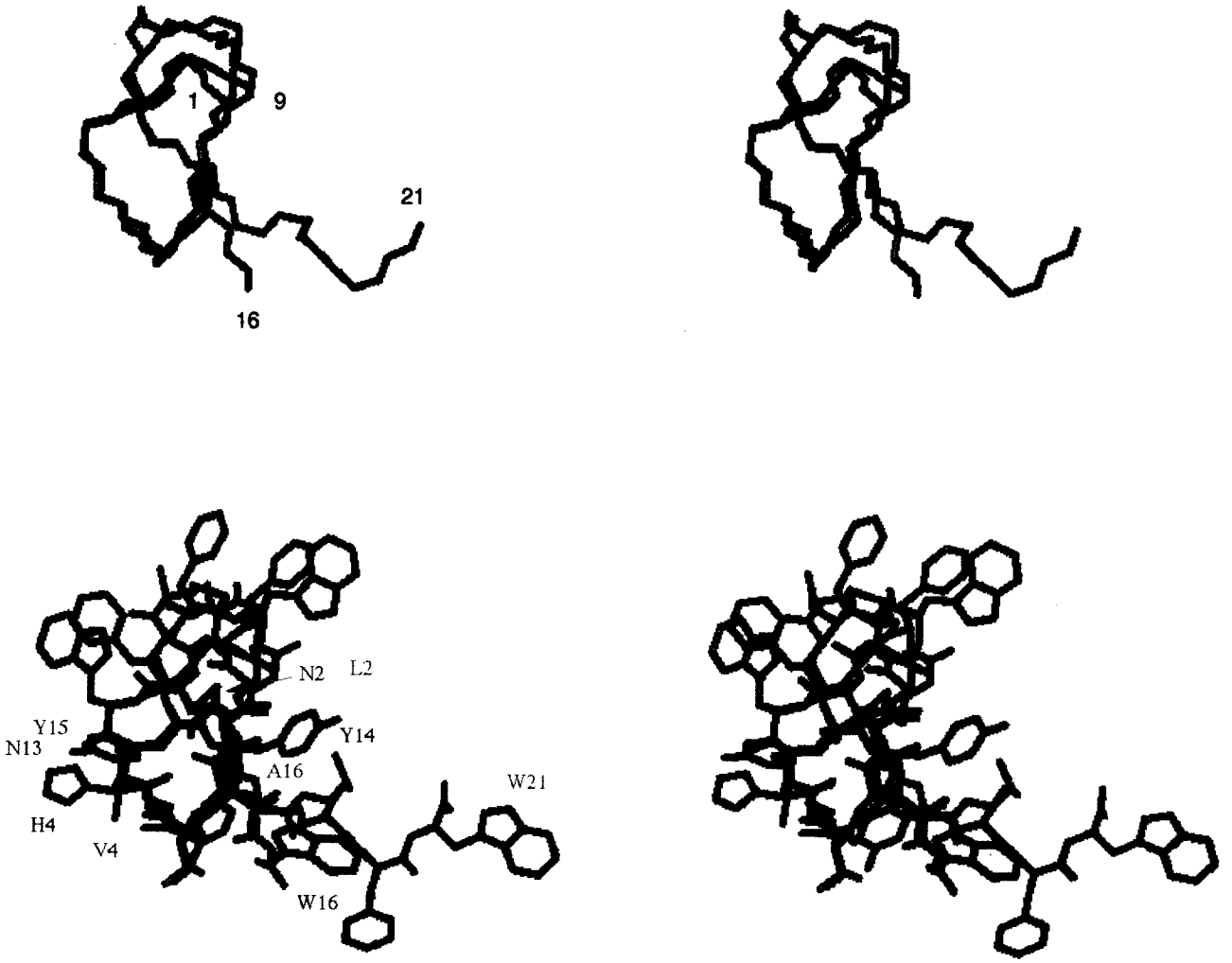

Figure 7. Stereoview of the superimposed structures of MS-271 (red) and RES-701-1 (purple). The structures were superimposed for minimum pairwise rms values of the Cα atoms (top, backbone atoms and bottom, heavy atoms).

corresponds to Tyr14, which is the next residue to Asn13 in the β-sheet of RES-701-1. Therefore the orientation of the side chain of residue 2 and the middle residue of the β-sheet region in the 'tail' in MS-271 was defined by the side chain–backbone NOEs, similarly to that of RES-701-1. In conjunction with the characteristic feature of the hydrogen bond indicated above, it is suggested that the backbone structure of the ring region (1–9) and three residues of the β-sheet segment in the 'tail' (Phe12–Tyr14 in RES-701-1 and Gly14–Ala16 in MS-271), and the side chain structure of residue 2 and the middle residue of the β-sheet region in the 'tail' (Asn13 in RES-701-1 and Tyr15 in MS-271) comprises the 'core structure' which is commonly observed for this type of 'lasso' structure. As shown in the 3-D structure of MS-271 in Figure 7, the side chains of Leu2, Val4, Ala16, Ile17 and Val18 lie below the 'ring' surface. Similarly, for RES-701-1, the side chains of Asn2, Tyr14, Tyr15 and Trp16 lie below the 'ring' surface (Fig. 7). The amino acid sequences in these regions exhibit diversity between two peptides, however, it is interesting to note that the side chains listed above in MS-271 are hydrophobic and those in RES-701-1 are hydrophilic. As indicated in the previous report, the 'tail' cannot pass through the 'ring' after its closure. Thus, it is considered that the 'ring' becomes closed on adequate folding of the peptide. Therefore, it is suggested that the side chain interaction of the residues indicated above may be responsible for the folding of the peptide which leads to the 'lasso' structure.

As suggested in the previous report,[7] RES-701-1 and MS-271 exhibit resistance to protease digestion even though they are very small peptides. Therefore it is suggested that the observed 'core structure' may be responsible for their resistance to protease digestion.

The factors which are not essential for folding into the 'lasso' structure

We next examined the unimportant factors as to folding into the 'lasso' structure on the basis of comparison between MS-271 and RES-701-1.

MS-271 possesses two disulfide bonds, different from RES-701-1. Since RES-701-1, which does not possess a disulfide bond, folds into the 'lasso' structure, the two disulfide bonds in MS-271 are not required for the folding into the 'lasso' structure.

The loop region between the β-sheet segments is composed of two residues in RES-701-1 and four residues in MS-271. The structural role of the loop region is to connect the β-sheet segment and thus it would not be responsible for the folding of the 'lasso' structure. It is suggested that the minimum structural requirement of the loop region is that it consists of two residues.

As indicated above, peptides which possess the same internal linkage as MS-271 and RES-701-1 are known, i.e. anantin[9] (Fig. 1) and propeptin[10] (Fig. 1), although the 3-D structures of these peptides have not yet been reported. For anantin, the number of residues comprising the 'ring' is one less than that of RES-701-1. For the 'lasso' structure, a large size 'ring' is not necessarily required. For example, the 'tail' of MS-271 passes through the 'ring' at the site between the CO of Tyr15 and NH of Ala16 (CO of Asn13 and NH of Tyr14 in MS-271), indicating that only a small space is required for the backbone to pass through the 'ring'. The diameter of the 'ring' is about 10–11 Å in MS-271 and RES-701-1. Thus, if the number of residues comprising the 'ring' is one less, it will not cause a serious steric interaction between the 'tail' and the 'ring'. Therefore, the 'ring' does not necessarily have to consist of nine residues. Anantin, which possesses a smaller size of 'ring', would fold into the 'lasso' structure. These two additional peptides may thus adopt this type of the 'lasso' structure and belong to this structural family.

Comparison of the structures of RP 71955, siamycin II and MS-271

The amino acid sequence of MS-271 is very similar to those of RP 71955 and siamycin II. The detailed structural information on RP 71955 obtained from the BrookHaven Protein Data Bank revealed that the feature of the 'lasso' structure indicated above is also observed in the structure of RP 71955. The rms value for Cα atoms of residues 1–19 between MS-271 and RP 71955 was 1.0 Å, indicating that the two structures are very similar. It is interesting to note that the 3-D structures of the 'ring' region and a part of the 'tail' region of MS-271 and RP 71955 are conserved in spite of the fact that different solvent systems were used for the experiments (RES-701-1 and MS-271 were investigated in DMSO by our group, and RP 71955 in a mixture of methanol/water by Frèchet et al.). For siamycin II, it was reported that a long-range NOEs were observed between the aromatic proton of Trp21 and the CαH and CβH of Cys7, and that the C-terminal 19–21 region was well determined[11] However, these NOEs were not observed in MS-271 and the C-terminal 19–21 region was not determined. The amino acid sequence of MS-271 differs at only one site from that of siamycin II (Val4 in MS-271 and Ile4 in siamycin II), and that position is in the 'ring' region. The amino acid replacement at position 4 in the 'ring' region is not responsible for the difference in the conformation of the C-terminal region. Thus, the difference in the C-terminal region is probably due to a difference in the increased hydrophobic interaction on the addition of H_2O in syamicin II.

In conclusion, we determined the solution structure of MLCK inhibitor MS-271, which possesses the same internal linkage as RES-701-1. The resulting structure was the 'lasso' structure, as observed in RES-701-1. As indicated in the previous report, the general structural motif of MS-271 and RES-701-1, the 'lasso' structure, would be a close representation of the bio-active

conformation since the 'tail' cannot pass through or pass back out once the 'ring' has been formed. A comparison between MS-271 and RES-701-1 revealed the features of this type of 'lasso' structure, which may be responsible for the backbone folding of the peptides which leads to the 'lasso' structure.

Experimental Procedure

NMR experiment

Since MS-271 could not be dissolved in 100% H_2, it was dissolved in deuterated dimethyl sulphoxide (DMSO-d_6) at a concentration of 3 mM. NMR spectra were recorded at 30 °C on BRUKER AM-500 and JEOL JNM-A400 spectrometers. Chemical shifts were referenced to the methyl proton resonance of DMSO at 2.5 ppm.

Two-dimensional nuclear Overhauser effect spectroscopy (NOESY),[13] double quantum-filtered shift correlated spectroscopy (DQF-COSY)[14] and homonuclear Hartmann–Harn spectroscopy (HOHAHA)[15] spectra in the phase sensitive mode using time proportional phase incrementation, and exclusive COSY (E.COSY)[16] spectrum in States mode were recorded, respectively. Spectra were normally collected with 512 complex points in the t_2 and 2048 complex points in the t_2 dimension. The t_2 FIDs were multiplied by a shifted sine-bell square window function and then Fourier transformed. The t_1 data were multiplied by the same window function, zero-filled to 2048 points, and then Fourier transformed. The NOESY spectra were collected with two mixing times, 100 ms and 300 ms. The NOESY spectrum with the longer mixing time was used for the signal assignments, and that with the shorter one was used to obtain the distance information. The $^3J_{NH\alpha}$ coupling constants were obtained from the DQF-COSY spectrum using the method of Kim and Prestegard.[17] The $^3J_{\alpha\beta}$ coupling constants were directly obtained from the E.COSY spectrum (0.85 Hz/point).

Calculations

In order to construct the ring conformation of MS-271, the chemical structure of Asp9 was modified by means of the MolEdit program in the MolSkop system (JEOL Co. Ltd.) on a TITAN computer. The intensities of the NOE cross peaks were classified into four categories by counting the contour levels, strong (2.5 Å), medium (3.0 Å), weak (3.5 Å), and very weak (4.0 Å). The 182 ^{1}H-^{1}H distance constraints (39 intra-residue, 71 inter-residue, 11 medium-range ($1 < i\text{-}j \leq$), and 61 long-range ($i\text{-}j \geq 4$) NOEs), 11 ϕ angles and 2 $\chi 1$ angles were used for the calculations. The distance constraints for the hydrogen bonds were not used in the calculations.

The solution structure was obtained by the combination of DG and SA calculations. DG calculations were carried out with the DADAS90 program[18] in the MolSkop system on a TITAN computer. Starting from the 100 initial structures with randomly chosen dihedral angles, the structures with the 40 best satisfied distance and angle constraints were obtained. SA calculations for refinement were carried out with the X-PLOR program[19] on an IRIS Indigo R4000 computer. The time step of dynamics was set at 5 fs during the SA calculations. Force constants for the NOE constraints and dihedral angle constraints were maintained at 50 kcal mol^{-1} Å^{-2} and 200 kcal mol^{-1} rad^{-2}, respectively, throughout the refinement process. The system was cooled stepwise from 1000 K to 100 K in 50 K decrements via 15 ps restraint dynamics, during which the repulsive term was increased linearly from 0.003 to 4 kcal mol^{-1} Å^{-4}. Final structures were obtained after 1500 cycles of Powell minimization. Finally, 35 well-converged structures were obtained.

The 3-D structure of RP 71955 was obtained from the Brookhaven Protein Data Bank.

References

1. Yano, K.; Toki, S.; Nakanishi, S.; Ochiai, K.; Ando, K.; Yoshida, M.; Matsuda, Y.; Yamasaki, M. *Bioorg. Med. Chem.* **1996**, *4*, 115.

2. Bylund, D. B. *Trends Pharmacol. Sci.* **1988**, *9*, 356.

3. Kobilka, B. K.; Matsui, H.; Kobilka, T. S.; Yang-Feng, T. L.; Francke, U.; Caron, M. G.; Lefkowitz, R. J.; Regan, J. W. *Science* **1987**, *238*, 650.

4. Helynck, G.; Dubertret, C.; Mayaux, J. F.; and Leboul, J. *J. Antibiotics* **1993**, *46*, 1756.

5. Frächet, D.; Guitton, L. D.; Herman, D.; Faucher, G.; Helynck, B.; du Sorbier, M.; Ridoux, J. P.; James-Surcouf, E.; Vuilhorgne, M. *Biochemistry* **1994**, *33*, 42.

6. Nishio, M.; Kawano, K.; Yamamoto, S.; Fukagawa, Y.; Oki, T. *J. Antibiotics* **1995**, *48*, 433.

7. Katahira, R.; Shibata, K.; Yamazaki, M.; Matsuda, Y.; Yoshida, M. *Bioorg. Med. Chem.* **1995**, *3*, 1273.

8. Katahira, R.; Shibata, K.; Yamazaki, M.; Matsuda, Y.; Yoshida, M. *Bioorg. Med. Chem. Lett.* **1995**, *5*, 1595.

9. Wyss, D. F.; Lahm, H-W.; Manneberg, M.; Labhardt, A. M. *J. Antibiotics*. **1991**, *44*, 172.

10. Ezumi, Y.; Itoh, Y.; Uramoto, M.; Kimura, K.; Gotou, M.; Yoshihama, M. *Nippon Nogeikagaku Kaishi*, **1992**, 460.

11. Constantine, K. L.; Friedrich, M. S.; Detlefsen, D.; Nishio, M.; Tsunakawa, M.; Furumi, T.; Ohkuma, H.; Oki, T.; Hill, S.; Bruccoleri, R. E.; Lin, P-F.; Mueller, L. *J. Biomol. NMR*, **1995**, *5*, 271.

12. Wüthrich, K. *NMR of Proteins and Nucleic Acids*; J. Wiley & Sons: New York, 1986, p 130.

13. Jeener, J.; Meier, B. H.; Bachmann, P.; Ernst, R. R. (1979) *J. Chem. Phys.* **1979**, *71*, 4546.

14. Rance, M.; Sorensen, O. W.; Bosenhausen, G.; Wagner, G.; Ernst, R. R.; Wuthrich, K. *Biochem. Biophys. Res. Commun.* **1983**, *117*, 479.

15. Branshweiler, L.; and Ernst, R. R. *J. Magn. Reson.* **1983** *53*, 521.

16. Griesinger, C.; Sorensen, O. W.; Ernst, R. R. *J. Am. Chem. Soc.* **1985**, *107*, 6394.

17. Kim, Y.; Prestegard, J. H. *J. Magn. Reson.* **1989**, *84*, 9.

18. Endo, S.; Wako, H.; Nagayama, K.; Go, N. In *Computational Aspects of the Study of Biological Macromolecules by Nuclear Magnetic Resonance Spectroscopy*; Plenum: New York. 1991, p 233.

19. Brünger, A. T. X-PLOR Version 3.1, User Manual, Yale University, New Haven, CT. 1990.

(*Received in Japan* 8 *August* 1995; *accepted* 27 *November* 1995)